Interaction of Wheelspace Coolant and Main Flow in a New Aeroderivative Low Pressure Turbine

F. Montomoli[1]
M. Massini[1]
N. Maceli
M. Cirri
L. Lombardi
A. Ciani
M. D'Ercole
R. De Prosperis

GE Infrastructure, Oil & Gas,
Via Matteucci 2,
Firenze, Italy

Increased computational capabilities make available for the aero/thermal designers new powerful tools to include more geometrical details, improving the accuracy of the simulations and reducing design costs and time. In the present work, a low-pressure turbine was analyzed, modeling the rotor-stator including the wheel space region. Attention was focused on the interaction between the coolant and the main flow in order to obtain a more detailed understanding of the behavior of the angel wings, to evaluate the wall heat flux distribution, and to prevent hot gas ingestion. Issues of component reliability related to thermal stress require accurate modeling of the turbulence and unsteadiness of the flow field. To satisfy this accuracy requirement, a full 3D URANS simulation was carried out. A reduced count ratio technique was applied in order to decrease numerical simulation costs. The study was carried out to investigate a new two-stage low-pressure turbine from GE Infrastructure Oil & Gas to be coupled to a new aeroderivative gas generator (the LM2500+G4) developed by GE Infrastructure, Aviation.
[DOI: 10.1115/1.3195036]

1 Introduction

The competitive nature of the gas-turbine market stimulates designers to consider a great number of design solutions to improve reliability and performance and to reduce life cycle costs. An accurate assessment of the relative contributions of the components of the gas-turbine engine is needed to achieve these goals. As a consequence, there is an increased trend to perform detailed analyses not only to ensure that the structural and performance requirements are fulfilled, but also to provide an accurate estimate of the life for each critical component. This approach must be followed in order to optimize maintenance service schedules or to upgrade an engine with consideration to residual life. From this point of view, the high-temperature operating environment of the gas-turbine plays a primary role, and heat transfer analysis becomes one of the most important steps in the design process.

When evaluating the heat load on a critical engine part, simplification of the geometry or operating conditions can seldom be made without paying a price in terms of accuracy or design margins, and very often leads to designs that do not meet the potential for optimum performance.

A number of publications on the subject of heat transfer can be found, in which the importance of the detailed reproduction of both geometry and boundary conditions has been stressed [1,2].

The cavity region between two adjacent blade-rows is a very complex one, and the increasing pressure ratios and cycle temperatures call for a balance between the two requirements of providing margin to avoid hot gas ingestion and for a reduction in purge flow. Prior studies dealing with these cavity flows have focused mainly on their aerodynamic effects. For example, McLean et al. [3,4] presented a detailed comparison of the mainstream aerodynamic effects due to several wheel space coolant injections. Hunter and co-workers [5,6] compared the results obtained with a source term approach and an unsteady solver to the experimental data available for a low-pressure turbine. Gier et al. [7] analyzed the details of the flow into a stator-rotor cavity and also presented an approach to separate the different loss mechanisms related to the shroud leakages. Cherry et al. [8] showed the overall performance decay due to endwall gaps, seals, and clearance together with experimental data. They all agree on the substantial effect of the secondary flow systems on engine performance. Among others, Forster et al. [9], Gentilhomme et al. [10], and Paniagua et al. [11] showed the importance of the circumferential pressure distribution near the cavity trench, of the proximity of the seal to the vane and blades, as well as of the unsteadiness due to the stator-rotor interaction for a reliable analysis of the hot gas ingestion through the rim seal system.

With regard to heat transfer, many authors have evaluated the Nusselt distribution in a rotating cavity or in a rotor-stator cavity [12], but to the authors' knowledge, a heat transfer analysis of a full rotor-cavity-stator model has not been published.

The turbine analyzed in this work, the LM2500+G4/PGT25 +G4 [13] is the fourth generation upgrade of the LM2500/PGT25 family, one of the most widely used aeroderivative gas-turbine for marine and industrial applications. The increased flow capacity of the LM2500+G4 gas generator, coupled with GE Oil & Gas upgraded high speed power turbine (HSPT) to make the PGT25 +G4, provides 33.9 MW with a thermal efficiency greater than 41%. The HSPT operative range is from 3050 rpm to 6400 rpm with a nominal speed of 6100 rpm.

Knowledge of aerothermal phenomena related to critical components plays a key role in blade life prediction. In this paper the effect of wake unsteadiness on the wheelspace region was analyzed numerically in order to evaluate the interaction with the coolant injection and to determine if local hot gas ingestion exists. In addition the influence of unsteadiness on the wall heat flux was evaluated.

[1]Present address: Whittle Laboratory, University of Cambridge, UK.

Contributed by the International Gas Turbine Institute of ASME for publication in the JOURNAL OF TURBOMACHINERY. Manuscript received May 21, 2009; final manuscript received June 3, 2009; published online April 2, 2010. Review conducted by David Wisler. Paper presented at the ASME Turbo Expo 2006: Land, Sea and Air (GT2006), Barcelona, Spain, May 8–13, 2006.

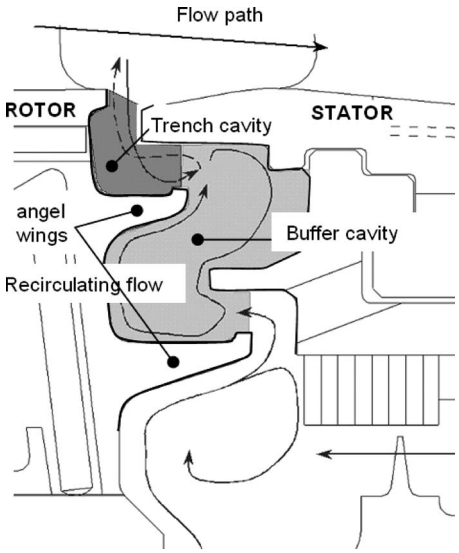

Fig. 1 Typical LPT wheel space

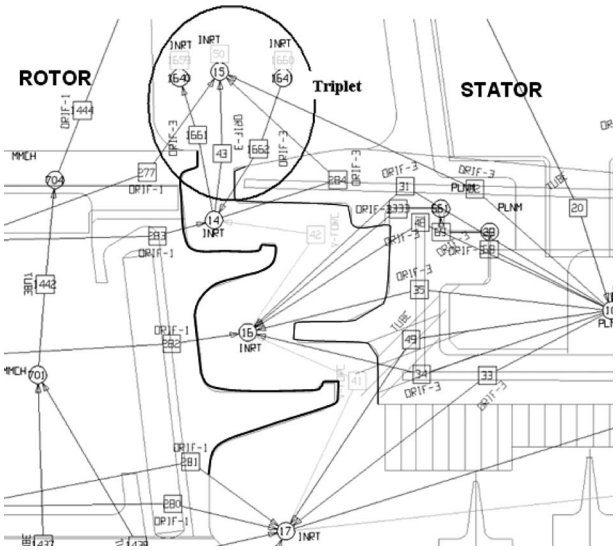

Fig. 2 YFT layout of triplets method

2 Problem Description

The mass flow used to purge the wheel space cavity has to satisfy two opposing requirements: assuring a margin for hot gas ingestion and maintain a high level of performance. The objective is to minimize the purge flow.

As a design practice the mass flow used to purge the cavity must accommodate hot gas ingestion but with the limitation that the ingested hot gas must be confined to the region before the upper angel wing to avoid reduced component life, as shown in Fig. 1.

The rotating disk surface causes the adjacent air to be driven outward by centrifugal forces. Figure 1 shows how the lower angel wing bends the cooling air from the radial direction, pushing it toward the diaphragm surface. In addition, a stable cold recirculation flow in the buffer cavity is designed to create a barrier for hot gas ingestion into the lower cavity

A circumferential static pressure gradient is always present at the vane interfaces in the flow path. The gradient intensity depends on the nature of the nozzles: with supersonic nozzles the trailing edge shocks produce very large pressure amplitude compared with subsonic nozzles.

The design of this region requires a substantial interaction between aero, heat, and mechanical designers. The process starts with an aerodynamic analysis of cold airfoils and an evaluation of leakages with cold gaps. From these analyses thermal and mechanical loads are derived, hence, thermal growths and mechanical deformations. These effects change the airfoil shape, and consequently an iterative process is required to arrive at the final geometry. In addition the coolant leakage alters the flow field locally and the performance of the gas-turbine globally.

In the HSPT design process, the aerodynamic optimization of the airfoils was performed using the in-house solver TACOMA [14,15], including the coolant leakages and injection as source terms at wall. This in-house solver was used to obtain the final geometry; conversely the analyses shown in this paper were obtained using the commercial ANSYS CFX solver.

The airfoil heat transfer coefficient is evaluated by postprocessing the Tacoma field with an in-house solver, HTC [16]. The secondary flows are evaluated using the YFT in-house solver [17] that models the coolant flows as a 1D flow network. The circumferential nonuniformities are taken into account using the so called "triplets method."

In this approach the 1D flow network is created to represent purging and leakage flows in the region under investigation. The flow path circumferential pressure gradient is collapsed into three pressure chambers, capturing the average flow path pressure and the "high" and "low" pressure regions. This arrangement models the nonuniform tangential coolant distribution, as well as the local hot gas ingestions. Figure 2 provides an example of the flow network in an Oil & Gas turbine.

The greatest approximation is that the unsteady interaction and the pumping effect generated by the wake passage are not modeled. In the HSPT design process, reliability and efficiency were the most important targets and necessitated a more detailed investigation of the behavior of flows in the wheel space to accurately predict blades life.

3 The Study Geometry and Boundary Conditions

The investigated domain includes the third stage rotor, the fourth stage stator vanes, and the rotor-stator cavity of the HSPT gas turbine, as shown in the cross section in Fig. 3. The analysis model considers the thermal growth of the components that affects the geometry of the flow path, blades, and wheel space. The wheel space region was accurately reproduced; it is possible to observe in Fig. 1 the classic GE shape of the angel wing with the lip turned up at the end; in the blade geometry the real fillets at the tip and hub are included.

Coolant injection in front of the rotor and leakages at the rotor dovetail were included in the BCs. Minor approximations on the

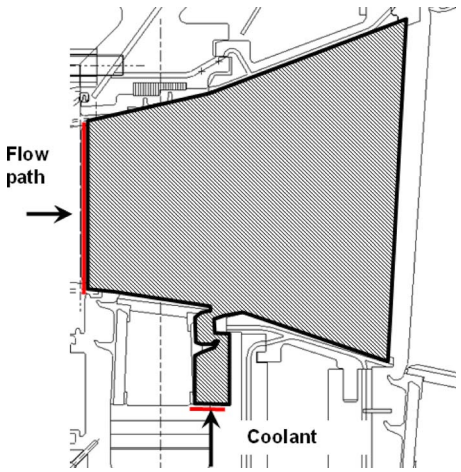

Fig. 3 Cold cross section without thermal growth effects

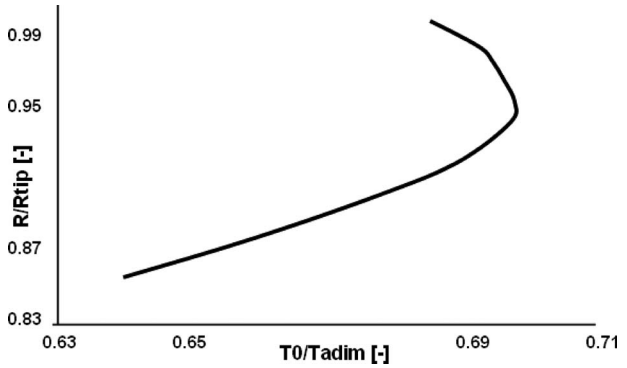

Fig. 4 Radial temperature distribution at flow path inlet

coolant leakages from the platforms into the main flow path were considered to be acceptable. The leakages and platform gaps were not included.

The investigated domain includes two inlets; the main inlet is upstream of the rotor and the second one models the flow cooling the wheel space analyzed. The distance between the inlet and outlet surfaces is different than that shown in Fig. 3. The drawing is the cold cross section without thermal effects.

The conditions imposed at the inlets are the stagnation quantities total pressure P_0, total temperature T_0, and the flow angles. The flow path data (total pressure distribution and the flow angles) are obtained from the through-flow calculation of the complete LM2500+G4 engine, but the radial temperature distribution upstream of the LPT is obtained from an experimental evaluation.

Figure 4 shows the radial temperature distribution used at the rotor inlet. The distribution includes the effect of the coolant leakages from the platforms and the coolant injection from the outer transition duct. The data are in nondimensional form using as reference the averaged total temperature at the LM2500+gas generator exit. The profiles are interpolated on the entire inlet surface and the tangential nonuniformities from the upstream stator are not included.

The analysis was performed for an LPT rotational speed of 6100 rpm. The wall temperature was set constant for the rotor and the stator was set with a no slip condition on the solid walls.

The BCs on the wheelspace region, swirl conditions, mass flow, pressure, and temperatures are obtained by modeling the secondary flows using the YFT solver. The solver analyzes the coolant redistribution in the entire region around the hot gas channel. These flows are called secondary flows to distinguish them from the main path.

The swirl velocities and angles are evaluated using the subroutine BJCAV that models the cavity pumping effects considering the real wheel space geometry.

Figure 5 shows the worm chart of the secondary flows obtained from the YFT analysis; the coolant leakages are expressed as a percentage of the compressor mass flow.

4 The Numerical Approach

The interaction of the wheelspace coolant with the main flow of the rotor-stator vanes were simulated with a computational fluid dynamics (CFD) analysis. 3D unsteady RANS simulations were performed with the CFX (ANSYS), Version 5.7.1 commercial unstructured code. The turbulence model is a standard two equations closure $k-\omega$ [18]; this is a common approach for CFD simulation in the industry.

The unstructured grids were generated in the domain by the grid generators, GAMBIT, Version 2.2 (Fluent Inc.) and ICEM-CFD, Version 5.1 (ANSYS). The meshes have triangular cells on solid surfaces, tetrahedrons in the core (generated by GAMBIT), and prismatic layers at the wall (generated by ICEM-CFD). The latter are

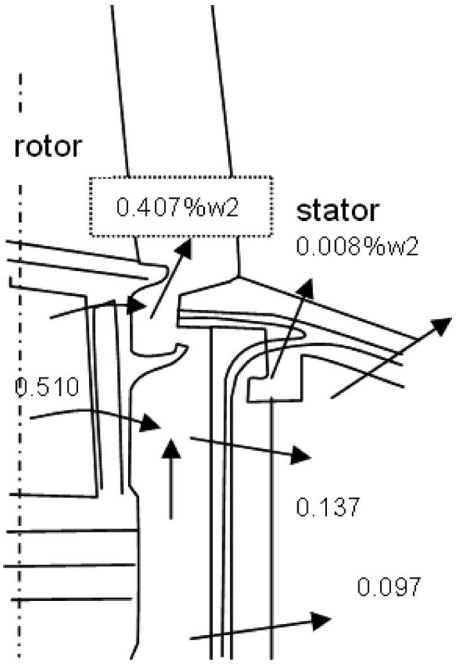

Fig. 5 Secondary flows worm chart

required to model the velocity gradients at the wall that are inherently anisotropic.

In the wheelspace region there are strong velocity gradients due to the presence of a rotating wall. This requires accurate node clustering near the solid surfaces.

The wheel space cavity and the stator hub are shown in Fig. 6(*a*); because of the strong velocity gradients due to the cross flow and the need to resolve the wake effect, this part was accurately discretized. In Fig. 6(*b*) the rotor tip is shown; here the geometry

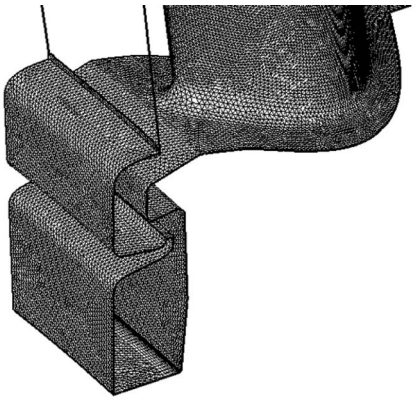

a) Wheel space region and stator

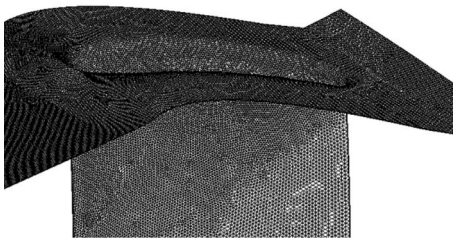

b) Rotor tip

Fig. 6 Surface meshes (*a*) wheel space region and stator and (*b*) rotor tip

has been simplified. The leakages up the tip shroud have not been modeled. This approximation is based on the assumption that the interaction between the wake passage and coolant is a local phenomenon not influenced by the injections at the tip.

The final mesh consists of more than 2×10^6 elements for the rotor vane with 10 prismatic layers, and 3.5×10^6 for the stator with 15 prismatic layers. The distance of the first node on the stator platform gives an average y+lower than 1. The prismatic layer growing law was set to 1.2.

The uneven rotor/stator ratio was modeled using the reduced count ratio technique; the ratio used in the present numerical computations is 1:1. The scaled vane is the stator vane in order to maintain the pitch of the incoming wake unaltered.

A steady mixing plane approach is used to assess the grid layout and to evaluate the grid sensitivity before the full 3D unsteady analysis of the flow field. The mixing plane for these previous calculations was placed upstream the cavity. The greatest approximation is that the pressure gradients generated by the rotor wake do not influence the coolant flow (are spanwise averaged by the mixing plane). The main advantage is that the flow gradients downstream of the cavity are better modeled, and the stator blockage effect is correctly detected. The second reasonable position, downstream the cavity, at the stator platform leading edge) was not used.

The mixing plane approach was abandoned for these simulations for the following two reasons.

- The interaction between the wake passage and coolant flow is inherently unsteady.
- The mixing plane averages the flow variables in the circumferential direction.

The fully 3D unsteady model is a time consuming approach but it is the only method to resolve this problem. In addition some flow features, such as the pulsating effect of the wake passage, is inherently unsteady and cannot be detected with different approaches.

Two different layouts were investigated: a 1.5 stage (complete third stage and nozzle of the fourth stage) and rotor-stator (without the nozzle of the third stage). For the unsteady setup the second configuration was preferred. Modeling a 1.5 stage the computational time increases and the mass flow, scaling the first nozzle to obtain the same pitch, dramatically decreases.

5 Numerical Results

One of the problems in unsteady simulation is how to analyze the results. More often, the variables, such as static temperature (and other energy related variables) or total pressure, are used to track the wake migration. The main approximation of this approach is related to a phenomenon called energy separation that occurs when a shear layer is present [19]. Energy separation consists of the isentropic rearrangement between total enthalpy and pressure in unsteady flows due to the presence of the pressure time derivative. A typical case is vortex shedding at the rotor trailing edge.

Numerically it is very difficult to accurately model this redistribution. This effect has very small spatial and temporal scales. Numerically this requires high computational time that is prohibitive for complex 3D geometries.

In the open literature some authors [20] have addressed this problem using a physical time step greater than the characteristic shedding period in unsteady simulations. It is presumed that the wake-coolant interaction and the shedding at the rotor trailing edge are decoupled in the frequency domain; so by filtering the Von Karman vortex street at the rotor exit, the main features of the wake-coolant interaction are still captured. In this paper the same approach is used, and the physical time step was not chosen to capture vortex shedding (in this case $f\cong100$ kHz) but is related to the passage frequency. The characteristic or passage frequency is obtained as the angular velocity (6100 rpm) divided by the angular pitch $(2*\pi/84)$.

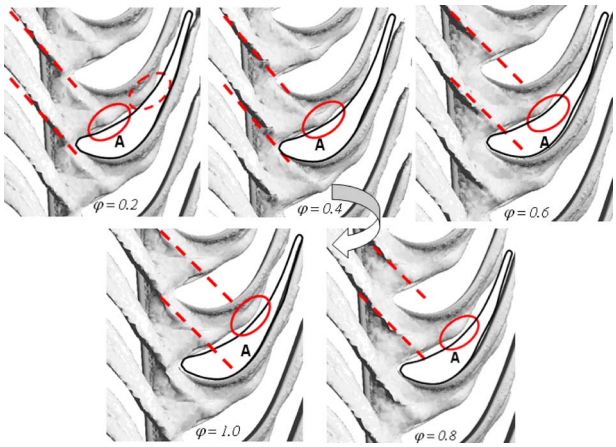

Fig. 7 Entropy isosurfaces at different time steps

To detect the flow features, the isosurfaces of static entropy are visualized. These surfaces are related to total pressure gradients (wakes) and total temperature gradients (coolant injection).

Physically, the coolant-wake interaction is a complex phenomenon involving potential interactions, (tangential pressure non uniformities), viscous interactions (coolant diffusion and turbulence transition), and acoustic interactions.

The first mechanism, called the potential effect, is related to the pressure fluctuations between the rotor and stator vane. The velocity defect in the wake region generates a nonuniform pressure distribution pitchwise. The circumferential nonuniformities affect the coolant injection, increasing the blowing ratio in the cavity under the wake. In addition the coolant ejected from the wheelspace has a blockage effect on the hot gas in the flow path [21]. The hot gas pressure recovery generates a pressure distribution from the cavity upstream edge (on the rotor platform) to the downstream edge (on the stator). The coolant is partially bent and this gradient enhances the coolant ejection. In this case it is not possible to predict a priori what the effect will be. The coolant mass flow is regulated by metering orifices but a rearrangement of leakages from the shanks and diaphragms is possible. In this simulation rearrangement is not possible because the leakages are not completely modeled.

Viscous interactions affect the heat transfer mechanism and the diffusion of coolant flow in the flow path. Viscous interaction is related to turbulence transition. The periodic passing of upstream wakes leads to transition patches on the downstream blade surfaces. This modification of the transition process is called "wake-induced" transition. The main effect is that when the upstream wake impinges on the downstream blade surface, within a laminar boundary layer, transition occurs because of the sudden and large disturbance caused by the wake and the high turbulence level inside the wake.

The acoustic interaction is connected to the first and second effect. The fluctuation of coolant flows generated by the wake passage propagates inside the wheelspace. The presence of a characteristic frequency related to the wheelspace geometry (volume and exit area) is expected.

In Fig. 7(*a*) the entropy isosurfaces at different time steps are shown. The time steps are arranged clockwise. The numerical sampling frequency is 213 kHz, and φ is the nondimensional time phase, evaluated as a fraction of the rotor period (instantaneous time/rotor period). It is possible to follow the wake migration in different time steps. In the position $\varphi=0.2$ the stator trims the wake and a pocket with a high entropy level is generated. The pocket is named A and marked with a red circle. Following the

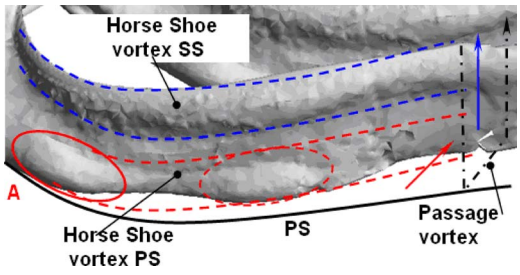

Fig. 8 3D entropy distribution at $\varphi=0.8$

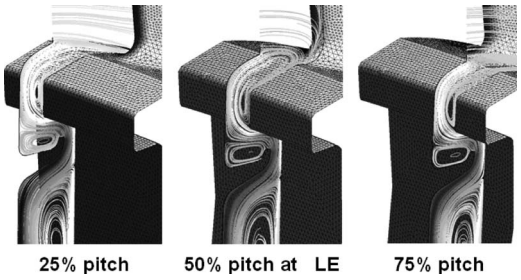

Fig. 11 Time averaged streamlines

time from $\varphi=0.2$ to $\varphi=1$ the pocket goes downstream embedded in the horseshoe vortex on the pressure side; reasonably, the horseshoe vortex, interacting with the passage vortex, pushes the pocket to the pressure side. At $\varphi=0.2$ the dashed circle indicates the pocket generated by the passage of the previous wake (or the position of the pocket A after the time period at $\varphi=1.2$).

Analyzing the 3D migration, as shown in Fig. 8, a spanwise migration of the secondary flows is observed. The horseshoe vortex on the SS interacts with the passage vortex and is lifted up to about the 30% of the span. At the same time the horse shoe vortex from the PS arrives on the SS but at a different span position, close to the hub (marked by dashed red lines). As suggested by Paniagua et al. [11], this effect may be increased by the coolant flow ejected from the cavity.

This can be confirmed by considering the total temperature distribution in a section close to the stator trailing edge (see Fig. 9). The coolant is entrained by the secondary flows, and from the thermal field the position of the relative core can be detected.

In a problem with coolant injection, whether the entropy is generated by temperature gradients or by total pressure variations is not easily distinguishable. For this reason in Fig. 10 the total pressure distribution at the same location as the temperature distribution of Fig. 9 (85% axial chord stator) is shown. From this

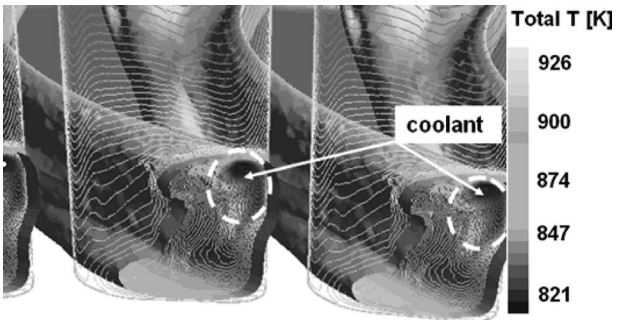

Fig. 9 Total temperature distribution at 85% axial chord of the stator vane

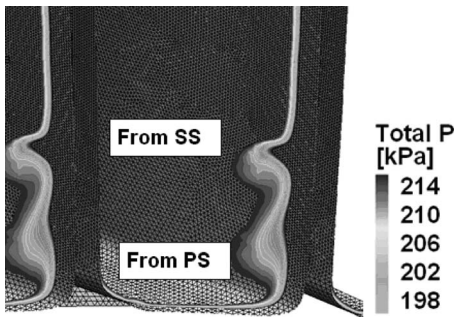

Fig. 10 Total pressure distribution at 85% axial chord of the stator vane

image, it is easier to detect the structure of the secondary flows. The total pressure distribution indicates more clearly the position of the horseshoe vortices arising from the stator PS and from SS (Fig. 11).

The design process requires that the hot gas ingestion, if present, must be confined to the first angel wing. Thus, the unsteady results were time averaged, and the streamlines at different locations are compared. The streamlines are obtained considering the velocity components on the cutting planes at three different angular locations 25%, 50% (stator LE), and 75% of the pitch angle. It is important to note that these structures are inherently 3D and that the main component is the tangential component. The swirl distribution ranges from 1, close to the rotor surface, to 0 at the stator diaphragm.

The time-averaged flow field solution shows the presence of three main recirculation bubbles. The lower bubble is generated by the rotating surface of the rotor pumping the gas radially and interacting with the angel wing. The second one is on the upper part of the angel wing. This recirculation bubble generates a flow structure that acts like a barrier and prevents hot gas ingestion. The angel wing shape with the end of the lip turned up increases and stabilizes this vortex. The third bubble could be responsible for hot gas ingestion. The recirculation is very small and confined to the region up to the angel wing. In front of the leading edge the bubble is bigger because the dynamic pressure recovery of the main flow increases the adverse pressure gradients seen by the coolant. On the contrary at 25% and at 75% of the pitch angle, on the pressure and suction sides, the bubble is smaller because the blockage effect is reduced. It appears useful to study the flow field with the cutting plane placed in front of the stator leading edge because the recirculation bubble is greater.

The propagation of the disturbance induced by the wake passage in the wheelspace cavity is one of the focal points of this study. In order to evaluate this unsteadiness, the effect the fluctuating field was analyzed. The velocity perturbation is obtained by subtracting the instantaneous and the ideal undisturbed fields. In this approach the wakes are visualized as negative jets. In a real 3D case it is difficult to define what the undisturbed ideal field is. In the open literature the most common approach is to consider the time average field as undisturbed.

The resulting field is a perturbed field where only the difference from the time-averaged solution is investigated. Figure 12 shows the instantaneous perturbed velocity vectors on a section plan placed at 50% of the pitch angle, in front of the stator leading edge. The cutting plane is placed in front of the leading edge because as already stated, it is the most critical location.

Two different time steps, $\varphi=0.6$ and $\varphi=1.0$, are investigated. At $\varphi=0.6$ the wake intersects the slicing plane at the wheel space exit. This increases the coolant ejection, reducing the recirculation bubble on the stator platform. The fluctuating vectors are directed outside the cavity.

When the opposite condition occurs, at $\varphi=1.0$, the fluctuating components are inverted; the coolant exit is in the middle of two consecutive wakes. There is a weak effect of this fluctuation on the global recirculation structure. The recirculation bubble is

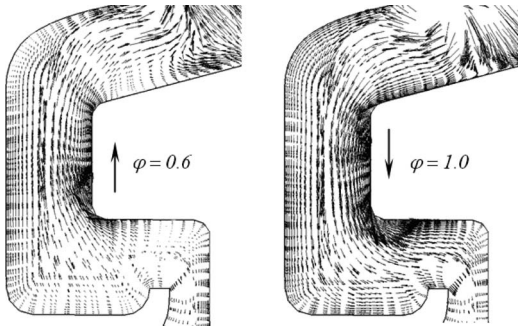

Fig. 12 Fluctuating field with a cutting plane intersecting the stator LE 50% of pitch angle

stronger but is still confined in the upper part of the stator platform; this effect was confirmed by the analysis of the instantaneous flow field.

The effect of the pulsating wake on stator heat transfer was evaluated considering the wall heat fluxes. The solid walls were treated as isothermal with an average metal temperature. The wall flux is considered positive when the walls warm the fluid. It is possible to isolate the effects of the wakes on the coolant considering only the positive component of the wall heat flux.

Figure 13 shows the isosurfaces on the stator surface at different time steps. The images are arranged clockwise. The coolant fluctuations on the suction side are clearly visible. From the position of the positive heat flux on the suction side it is possible to conclude that the main effect is due to the coolant embedded in the horseshoe vortex on the SS. This is confirmed by the total temperature distribution shown in Fig. 9. When the coolant entrained in the horseshoe vortex reaches the SS, the mixing with the hot gas increases the global temperature, and the effect of this migration is not clearly visible.

Finally, the effect of wake passage was evaluated on the vane surface (Fig. 14). The dashed red lines indicate the wake position at every time step. The coolant is stable on the vane hub, and only a small fluctuation can be detected on the platform nose; the quantitative amplitude of this fluctuation on the platform, at two different locations, is shown in Fig. 15. This small fluctuation can be explained considering that the coolant flow is uniform and major hot gas ingestion is not present.

This confirms the robustness of the design because with a reduced coolant mass flow, it is possible to assure uniform purging of the wheel space cavity. The only critical recirculation bubble is confined to the upper part of the wheel space on the nozzle platform.

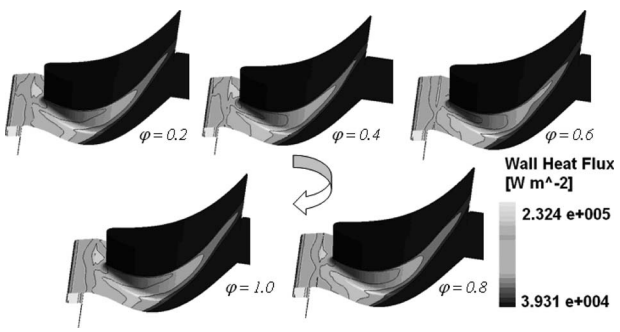

Fig. 13 Positive wall heat flux (flow colder than the solid surface)

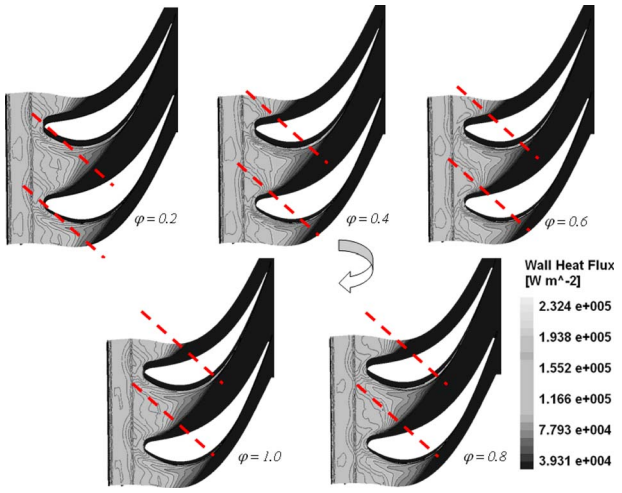

Fig. 14 Positive wall heat flux (flow colder than the solid surface)

6 Conclusions

The importance of the study is related to the flow investigation in a real case (PGT25+HSPT), evaluating the unsteady effect from aerodynamic and thermal point of view. The geometry was obtained, taking into account thermal growth. The BCs arise from the numerical models (throughflow calculation of the complete turbine) and from experiment (radial temperature distribution). The CFD simulation shown in this paper adds a new contribution to the design process.

A strong interaction is shown between secondary flows, horseshoe and passage vortex, and coolant. The coolant ejected from the wheelspace is embedded in the horseshoe vortex and is collected on the suction side.

The coolant purging flows and the wheelspace geometry are able to prevent hot gas ingestion under all conditions. Only a small recirculation bubble is placed on the platform leading edge. The flow field in the wheel space confirms the good design of the angel wings that generates a stable recirculation bubble preventing the hot gas ingestion. The analysis of the disturbance field shows a pulsating effect generated by the wake passage but shows that there is no flow inversion.

From the thermal point of view, the positive wall heat flux was analyzed. The wall values were used to detect only the effects of the wake passage on the coolant flows. A fluctuation behind the wake passage was detected with stronger effects on the stator suction side, where the coolant flow is collected.

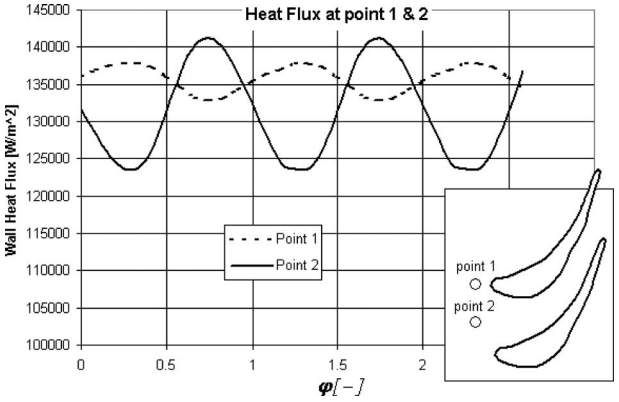

Fig. 15 Wall heat flux at points 1 and 2

On the stator vane, the coolant flow is stable on the platform surface, and high fluctuations of heat flux are not detected.

Unsteady simulations confirm the robustness of the design of the wheel space cavity between the third and fourth stage of PGT25+HSPT.

Future work will be based on the comparison of CFD results with experimental data from prototype tests.

Acknowledgment

Many thanks to all the GE businesses, which have cooperated in the LM2500+G4/PGT25+G4 project: GE Infrastructure's Aviation, Energy, and Oil & Gas.

The authors would like to thank L. Tognarelli, chief of Oil & Gas gas turbine engineering, for making this work possible.

References

[1] Garg V. K., 2001, "Heat Transfer in Gas Turbine," NASA, Report No. NASA/CR-2001-210942.
[2] Dunn, M., 2001, "Convective Heat Transfer and Aerodynamics in Axial Flow Turbines," ASME Paper No. 2001-GT-0506.
[3] McLean, C., Camci, C., and Glezer, B., 2001, "Mainstream Aerodynamic Effects Due to Wheelspace Coolant Injection in a High-Pressure Turbine Stage, Part I: Aerodynamic Measurements in the Stationary Frame," ASME Paper No. 2001-GT-0119.
[4] McLean, C., Camci, C., and Glezer, B., 2001, "Mainstream Aerodynamic Effects Due to Wheelspace Coolant Injection in a High-Pressure Turbine Stage, Part II: Aerodynamic Measurements in the Rotational Frame," ASME Paper No. 2001-GT-0120.
[5] Hunter, S. D., and Orkwis, P. O., 2000,"Endwall Cavity Flow Effects on Gaspath Aerodynamics in an Axial Flow Turbine: Part II—Source Term Model Development," ASME Paper No. 2000-GT-513.
[6] Hunter, S. D., and Manwaring, S. D., 2000, "Endwall Cavity Flow Effects on Gaspath Aerodynamics in Axial Flow Turbine: Part I—Experimental and Numerical Investigation," ASME Paper No. 2000-GT-651.
[7] Gier, J., Stubert, B., Brouillet, B., and de Vito, L., 2003, "Interaction of Shroud Leakage Flow and Main Flow in a Three-Stage LP Turbine," ASME Paper No. GT-2003-38025.
[8] Cherry, D., Wadia, A., Beacock, R., Subramanian, M., and Vitt, P., 2005, "Analytical Investigation of a Low Pressure Turbine With and Without Flowpath Endwall Gaps, Seals and Clearance Features," ASME Paper No. GT2005-68492.
[9] Förster, I., Martens, E., Friedl, W., and Peitsch, D., 2001, "Numerical Study of Hot Gas Ingestion Into an Engine Type High-Pressure Turbine Rotor-Stator Cavity," ASME Paper No. 2001-GT-0114.
[10] Gentilhomme, O., Hills, N. J., Turner, A. B., and Chew, J. W. 2002, "Measurement and Analysis of Ingestion Through a Turbine Rim Seal," ASME Paper No. GT-2002-30481.
[11] Paniagua, G., Dénos, R., and Almeida, S., 2004, "Effect of the Hub Endwall Cavity Flow on the Flow-Field of a Transonic High-Pressure Turbine," ASME Paper No. GT2004-53458.
[12] Evans, J., Stevens, L. M., Bodily, C., and Kang, M. B., 2004, "Prediction of Velocities and Heat Transfer Coefficients in a Rotor-Stator Cavity," ASME Paper No. GT2004-53639.
[13] Badeer, G. H., 2005, "GE's LM2500+G4 Aeroderivative Gas Turbine for Marine and Industrial Applications," GE Energy, Paper No. GER-4250.
[14] Tallman, J. A., 2004, "CFD Heat Transfer Predictions for a High-Pressure Turbine Stage," ASME Paper No. GT2004-53654.
[15] Tolpadi, A. K., Tallman, J. A., and El-Gabry, L., 2005, "Turbine Airfoil Heat Transfer Predictions Using CFD," ASME Paper No. GT2005-68051.
[16] Ciani, A., 2001, "Development of a Multizone Software for the HTC Prediction on Gas Turbine Blades," GE Nuovo Pignone, NPGE-HTC Manual.
[17] Laverty, W. F., 2003, Technical Manual GE Aircraft Engine, YFT, Jun.
[18] Wilcox, D. C., 1993, Turbulence Modeling for CFD, DWC Industries, Inc.
[19] Han, B., Goldsteint, R. J., and Choi, H. G., 2002, "Energy Separation in Shear Layers," Int. J. Heat Mass Transfer, **45**, pp. 47–55.
[20] Adami, P., Montomoli, F., Belardini, E., and Martelli, F., 2004, "Interaction Between Wake and Film Cooling Jets: Numerical Analysis," ASME Paper No. GT2004-53178.
[21] Montomoli, F., 2005, "Physics of Gas Turbine Cooling: Improvement of Design Tools," Ph.D. thesis, Department of Energetic "S. Stecco," University of Florence, Italian National Library.